Four-electron Electrocatalytic O₂ Reduction by a Ferrocene-

modified Glutathione Complex of Cu

Profulla Mondol and Christopher J. Barile*

Department of Chemistry, University of Nevada, Reno, Nevada 89557, USA

*Corresponding author: cbarile@unr.edu

Abstract

In this manuscript, we design non-precious metal electrocatalysts for the O₂ reduction

reaction (ORR) based on Cu complexes of the tripeptide glutathione modified with ferrocene

(Cu-GSH-NHFc). Homogenous catalysis experiments demonstrate that the covalently bound Cu-

GSH-NHFc catalyst exhibits enhanced activity as compared to mixtures of the individual catalyst

components. Heterogeneous catalysis results on rotating disk electrodes (RDE) and rotating

ring-disk electrodes (RRDE) show that Cu-GSH-NHFc catalyzes the ORR via a four-electron

pathway at pH 4-7, while the same catalyst without ferrocene produces significant quantities of

H₂O₂. Cyclic voltammetry reveals electronic coupling between the appended ferrocene moieties

and the Cu active site. From these studies, we propose an ORR reaction pathway in which fast

electron transfer facilitated by ferrocene explains the high selectivity of the Cu-GSH-NHFc

catalyst. We envision that this understanding will lead to future developments in the design of

non-precious metal ORR catalysts, which are instrumental to fuel cell technologies.

Keywords: Oxygen reduction reaction, non-precious metal catalysts, copper complexes,

glutathione, electrocatalysis.

1

Introduction

Energy conversion technologies mediated by electrocatalysis are pivotal in transitioning to a clean and renewable energy economy.^{1–7} Fuel cells are a promising technology that could play a critical role in this transition. Although the fuels utilized at the anode vary, the O₂ reduction reaction (ORR) occurs at the cathode in almost every fuel cell design. Through the ORR, a molecule of O₂ reacts with four protons and four electrons to yield two molecules of water. The performance of fuel cells is largely limited by the high overpotential needed to drive the ORR.⁸

Over the last forty years, a wide range of ORR electrocatalysts have been developed in an attempt to decrease the overpotential of this reaction. Pt-based materials and laccase enzymes are the catalysts that exhibit the lowest overpotentials. However, the high cost and scarcity of Pt and the low current densities of laccases hinder their widespread use as ORR catalysts. For these reasons, the development of stable, active, and earth-abundant ORR catalysts is an ongoing grand challenge.

Non-precious metal ORR catalysts, particularly those comprised of Fe or Cu complexes with nitrogen-rich ligands, are actively being studied as practical alternatives to Pt and laccases. For example, Fe complexes with porphyrins or other nitrogen-containing macrocycles have been explored for decades as promising catalysts. More recently, Cu catalysts have been investigated for the ORR. One promising class of Cu catalysts are those based on dinuclear Cu complexes with triazoles, which possess a similar overpotential to Pt, but suffer from poor durability. Additionally, Cui et. al prepared single atom Cu catalysts by pyrolyzing Cu phthalocyanine. In alkaline media, these materials catalyze the ORR at an overpotential that is 30

mV lower than a commercial Pt/C catalyst.²² Recently, Lu et. al demonstrated that electron density on the d orbitals of Cu weakens the O-O bonds, which results in the high ORR activity of Cu complexes.²³

We were inspired to use Cu complexes of glutathione to develop a new class of non-precious metal ORR catalysts. Glutathione is a tripeptide and nitrogen-rich ligand that is known to bind Cu ions in a wide variety of coordination environments. Additionally, the ability of glutathione to be oxidized and reduced via the thiol/disulfide couple increases the chemical diversity of these complexes through, for example, the formation of dimers. Previous work has also shown that glutathione can be modified with a range of pendant species such as quantum dots and ferrocene for use in a multitude of applications. ²⁶⁻²⁸

In this manuscript, we evaluate the ORR activity of Cu complexes of glutathione and glutathione covalently bound to a pendant ferrocene moiety. By increasing the electron transfer rate to the Cu active site, the complex with bound ferrocene catalyzes the ORR via four electrons to water. From these experiments, we propose a reaction pathway for ORR by these complexes that invokes the differential rates of electron and proton transfer to explain differences in the reactivities of the Cu complexes with and without bound ferrocene.

Experimental Methods

General Procedures. The synthesis of GSH-Fc is described in the "Synthesis of GSH-NHFc" section. All other chemicals were obtained from commercially available sources and used directly in experiments without further purification. A VSP-300 Biological potentiostat was used for all electrochemical studies. All electrochemical studies were performed in a three-electrode system in which modified glassy carbon, a graphite rod, and Ag/AgCl/3 M KCl (eDaq, Inc.) were the working, counter, and reference electrodes, respectively. Prior to use, glassy carbon

working electrodes were polished using a suspension of $0.05~\mu m$ alumina followed by sonication for 10 minutes in water.

Homogeneous Catalysis. The solution for homogeneous catalysis was prepared using 1 mM CuSO₄, 1 mM GSH-Fc, and 100 mM tetrabutylammonium perchlorate (TBAClO₄) in 70% MeOH and 30% water. This solution (5 mL) was used in each electrochemical cell and sparged with O₂ or N₂ for 7 minutes prior to running voltammetry.

Heterogeneous Catalysis. GSH-Fc (5.0 mg), CuSO₄ (3.0 mg), carbon (5.0 mg, Vulcan XC-72), MeOH (5.0 mL), and Nafion solution (25 μL, 5 wt.%, D520, Fuel Cell Store, Inc.) were added to a vial. The resulting mixture was sonicated for 10 minutes to yield a homogeneous suspension. About 80 μL of the suspension was drop-cast on a glassy carbon electrode (5 mm in diameter) and dried under ambient conditions using a custom-built upright rotator at a rotation speed of 8 rpm. This modified electrode was then used as the working electrode for rotating disk electrode and rotating ring-disk electrode experiments using an electrode rotator (MSRX, Pine Research, Inc.). Unless noted otherwise, Britton-Robinson buffers (40 mM H₃BO₃, 40 mM H₃PO₄, 40 mM CH₃COOH) were used and adjusted to the desired pH using NaOH. Voltammetry was performed with 45 mL of buffer solution sparged with O₂ for at least 7 minutes.

UV-Visible Spectroscopy. Solutions with a total concentration of 5 mM in DMSO contained CuSO₄ and GSH-Fc, GSH, or GSSG in DMSO. The molar ratio between the two components was varied for each trial, and the absorbances versus a DMSO solvent blank were recorded using quartz cuvettes with a path length of 0.1 cm and a Shimadzu UV-2550 spectrometer.

ICP-MS studies. GSHNHFC was dissolved in EtOAc (3 mM), and an aqueous CuSO₄ solution (6 mM) with the same volume was added to the GSHNHFc solution. Cu-GSHNHFc formed in the organic layer, which was separated from the aqueous layer and subsequently dried with

anhydrous Na₂SO₄. The solvent was then removed under vacuum, and ICP-MS analysis was conducted to quantify the Cu and Fe in the complex.

Synthesis of GSH-NHFc. The synthesis of GSH-NHFc was accomplished in four steps starting from GSSG. Boc-GSH was first synthesized in two steps from GSSG following established methods from the literature except the equivalents of di-t-butyl dicarbonate were increased by three times.²⁹ Next, to synthesize Boc-GSH-NHFc, Boc-GSH (0.10 g, 0.25 mmol) was dissolved in DMSO (20 mL) and Et₃N (0.12 mL, 3.0 mmol), HBTU (0.532 g, 1.32 mmol), and aminoferrocene (0.055 g, 0.274 mmol) were added. This mixture was continuously stirred for 18 hours at room temperature. The mixture was then diluted with EtOAc (200 mL) and washed with water (200 mL) followed by brine (3x 200 mL). The organic layer was dried over anhydrous Na₂SO₄, filtered, and removed under vacuum. The crude product was purified by flash chromatography on silica (ethyl acetate: hexane = 2:1, $R_f = 0.5$) to yield Boc-GSH-Fc (32 mg, 22% yield) with a ¹H NMR spectrum similar to literature. ²⁶ Finally, we deprotected the amino group from Boc-GSH-Fc to yield GSH-NHFc according to a literature method.²⁶ ¹H NMR (DMSO-d₆) δ 5.07 (s, 2H, H-3', H-4', Fc), 5.02 (s, 5H, unsubstituted Fc), 4.99 (s, 2H, H-2', H-5', Fc), 4.95 (t, 1H, CysCH), 4.20 (s, 2H, GlyCH₂), 3.51 (t, 1H, GluCH), 3.24 (d, 2H, CysCH₂), 2.17 (m, 4H).

Results and Discussion

Voltammetric Studies

We first synthesized a conjugate of glutathione and ferrocene (GSH-NHFc, Figure 1) in four steps following procedures modified from the literature. We then used cyclic voltammetry (CV) to evaluate the redox properties of glutathione (GSH), GSH-NHFc, and their Cu complexes. A CV of GSH-NHFc dissolved in a solution containing MeOH, water, and a

TBAClO₄ supporting electrolyte exhibits one redox coupling with a midpoint potential ($E_{1/2}$) of about 0.33 V vs. Ag/AgCl (Figure 2, black line). This couple is due to the Fe³⁺/Fe²⁺ redox and not the glutathione moiety because a control experiment with GSH shows no redox activity (Figure S1, black line).

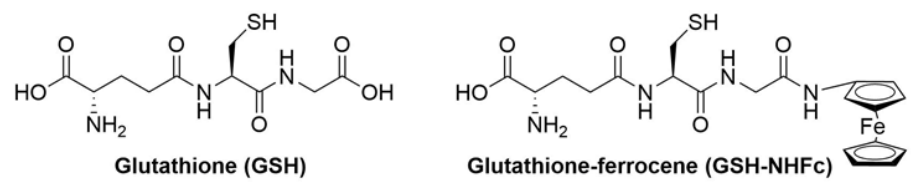


Figure 1: Structures of ligands used in this study.

The red line in Figure 2 shows a CV with 1 equivalent of CuSO₄ added to the GSH-NHFc solution. Compared to the CV of the solution without CuSO₄ (black line), the magnitude of the current density increases. In fact, the integrated charge under the redox waves approximately doubles (7.0 μC without Cu and 15.5 μC with Cu for the anodic peaks). This finding suggests that the redox wave with Cu is due to two electrons being transferred through the Cu²⁺/Cu⁺ and Fe³⁺/Fe²⁺ processes. A control experiment with CuSO₄ without GSH-NHFc only shows a redox couple with a very small amount of current density (Figure S1, red line). The differences between the CuSO₄ CVs with and without GSH-NHFc suggest that CuSO₄ forms a Cu complex with GSH-NHFc, which we denote as Cu-GSH-NHFc. The formation of a Cu complex is also confirmed by UV-visible spectroscopy experiments (*vide infra*).

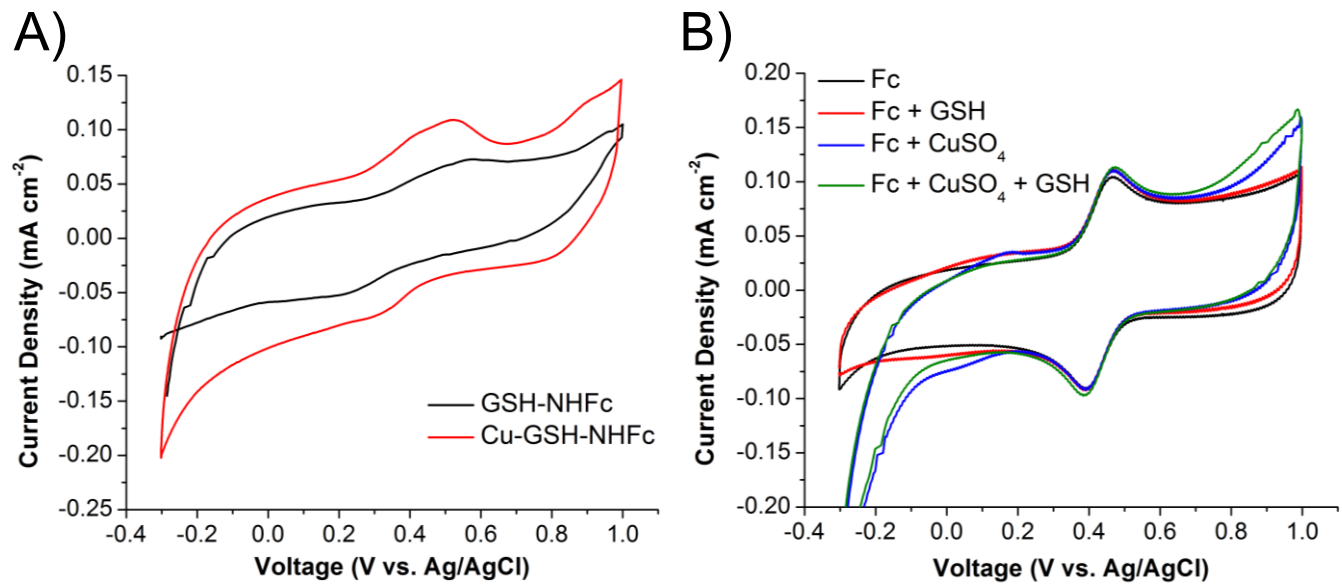


Figure 2: Cyclic voltammograms of a glassy carbon electrode at a 500 mV s⁻¹ in solutions containing 100 μM GSH-NHFc (A, black line), 100 μM Cu-GSH-NHFc (A, red line), 100 μM ferrocene (B, black line), 100 μM ferrocene and 100 μM GSH (B, red line), 100 μM ferrocene and 100 μM CuSO₄ (B, blue line), and 100 μM ferrocene, 100 μM CuSO₄, and 100 μM GSH (B, green line). All solutions also contained 70% MeOH and 30% aqueous 100 mM TBAClO₄.

To analyze the effect of having a glutathione moiety covalently bound to ferrocene, we studied CVs of free ferrocene and GSH. A CV of free ferrocene by itself contains one reversible redox couple with an $E_{1/2}$ value of 0.430 ± 0.01 V (Figure 2B, black line), which matches literature values. Adding glutathione to the ferrocene solution does not significantly alter the ferrocene CV (Figure 2B, red line). This result indicates that the covalent nature of the GSH-NHFc system causes it to exhibit significantly different electrochemical behavior as compared to a solution containing free ferrocene and free GSH. In particular, the $E_{1/2}$ value of free ferrocene is 0.06 V more positive than that of GSH-NHFc (0.370 ± 0.10 V). This positive shift in redox potential is due to the electron donating nature of the amide linkage of GSH-NHFc.

CVs of free ferrocene and $CuSO_4$ with and without GSH (Figure 2B, blue and green lines) also display the Fe^{2+}/Fe^{3+} redox couple at 0.43 V. In addition, these CVs contain a weak Cu^+/Cu^{2+} couple with an $E_{1/2}$ value of about 0.1 V that is similar to those observed in CVs of

CuSO₄ by itself and CuSO₄ with only GSH (Figure S1, red and blue lines). The similarity of the Cu^+/Cu^{2+} couples with and without free ferrocene indicates that the Fe^{2+}/Fe^{3+} couple in ferrocene and the Cu^+/Cu^{2+} couple are largely independent from one another unlike in Cu-GSH-NHFc. These results imply that the covalent nature of Cu-GSH-NHFc allows for electronic interactions between the Fe^{2+}/Fe^{3+} and Cu^+/Cu^{2+} redox couples. Electronic interactions between these two metal centers have previously been identified in other ORR catalysts with covalently-linked Fe and Cu sites. 31,32

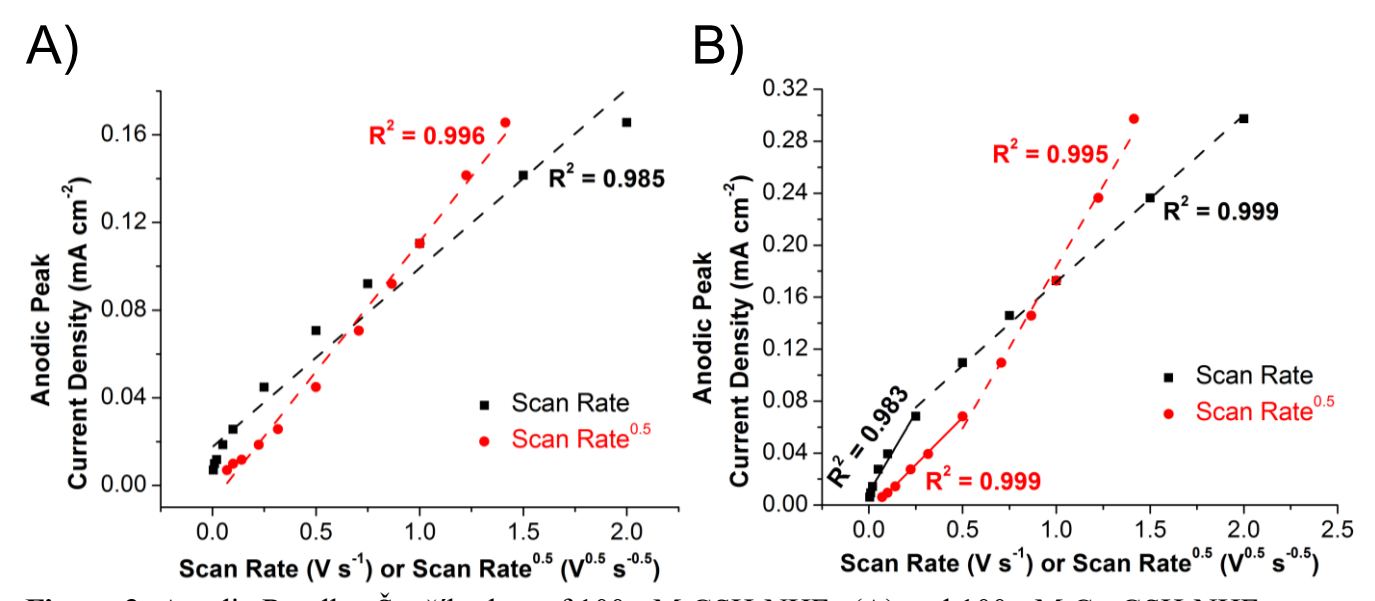


Figure 3: Anodic Randles-Ševčík plots of 100 μ M GSH-NHFc (A) and 100 μ M Cu-GSH-NHFc (B) in 70% MeOH and 30% aqueous 100 mM TBAClO₄.

Further evidence of electronic coupling between the two redox couples in Cu-GSH-NHFc can be gleaned from Randles-Ševčík analysis. Figure S2 shows Randles-Ševčík plots for the anodic and cathodic peak current densities of CVs of free ferrocene as a function of scan rate. As expected, a better linear fit is obtained when the data are plotted versus the square root of the scan rate as opposed to the scan rate. As observed previously,³³ this result indicates that free ferrocene diffuses to and from the electrode surface during the CVs and is not bound to the

electrode. Analogous experiments with GSH-NHFc show the same trend (Figures 3A and S3A), which also indicate that the GSH-NHFc molecule undergoes diffusion during its redox.

Interestingly, a different trend is observed in the Randles-Ševčík analysis of Cu-GSH-NHFc (Figures 3B and S3B). At slow scan rates (≤ 250 mV s⁻¹), a better linear fit is obtained when the data are plotted versus the square root of the scan rate as is observed for free ferrocene and GSH-NHFc. However, at fast scan rates (≥ 250 mV s⁻¹), the data is linear with respect to the scan rate. We hypothesize that at faster scan rates intramolecular electron transfer within Cu-GSH-NHFc results in a quasi-reversible redox, which is perhaps mediated by electrode absorption, resulting in the observed nonlinearity with respect to the square root of the scan rate. Regardless, these findings demonstrate that the electrochemistry of Cu-GSH-NHFc is more complex than that of free ferrocene or GSH-NHFc and that this complexity arises from the covalent linkage of the two redox couples.

Homogeneous Oxygen Reduction Catalysis

Having established the differences in electrochemistry between Cu-GSH-NHFc and its individual components, we next evaluated the ability of Cu-GSH-NHFc to electrocatalyze the ORR. A CV of an O₂-sparged solution containing Cu-GSH-NHFc exhibits enhanced cathodic current density compared to a control experiment with a N₂-sparged solution (Figure 4A). These results indicate that Cu-GSH-NHFc is a competent ORR electrocatalyst. Furthermore, the onset potential for O₂ reduction, defined here as the potential of the negative-going scan at which the current density reaches 10% of its maximum value, is -0.29 V vs. Ag/AgCl. This onset potential is comparable to those observed with previously reported Cu-based molecular ORR catalysts. A CV under the same conditions with GSH-NHFc yields a lower quantity of cathodic current and a more negative onset potential as compared to the CV of Cu-GSH-NHFc (Figure 4B, blue

line). This finding demonstrates that the presence of Cu aids in the ORR electrocatalysis. Moreover, a CV of a mixture of the three individual free components of Cu-GSH-NHFc (e.g. ferrocene, CuSO₄, and GSH) also exhibits less cathodic current and a more negative onset potential (Figure 4B, red line). This result demonstrates that these three components must be covalently linked to achieve superior ORR activity. Lastly, CVs of any one or two individual components also result in significantly less cathodic current compared to Cu-GSH-NHFc (Figure S4), which further reveal the superior electrocatalytic properties of Cu-GSH-NHFc.

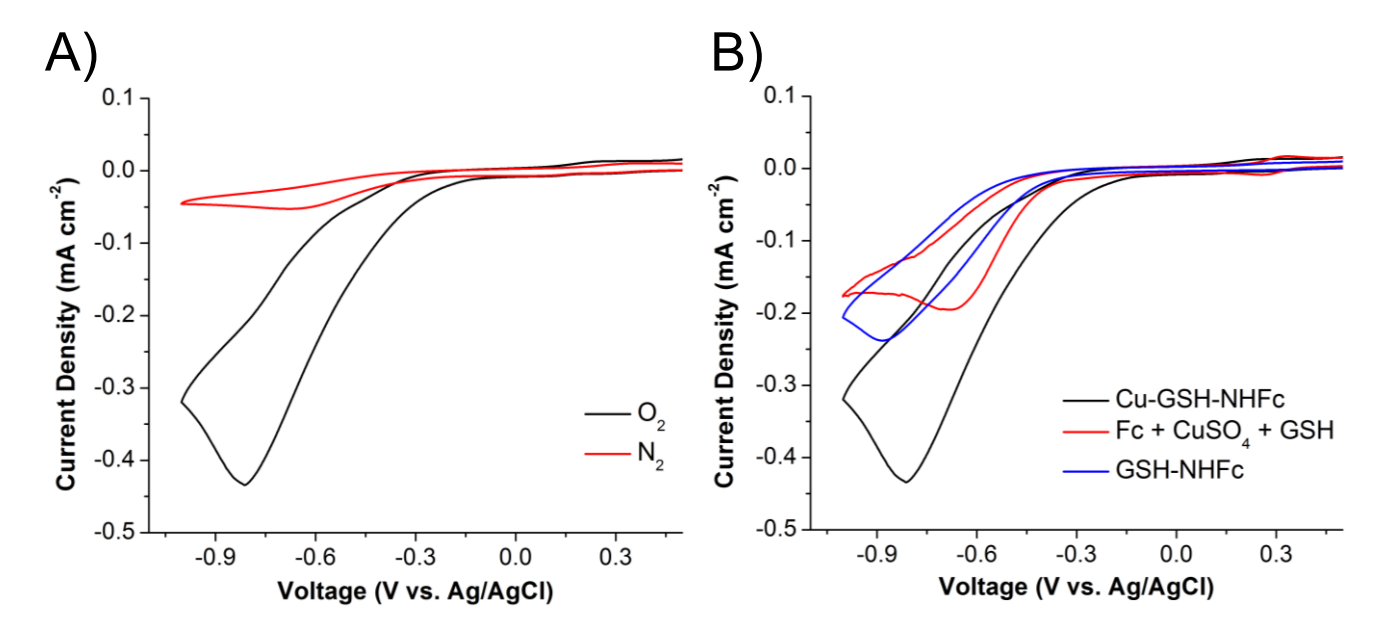


Figure 4: Cyclic voltammograms of electrocatalytic O_2 reduction on a glassy carbon electrode at a scan rate of 10 mV s⁻¹ in solutions containing 100 μM Cu-GSH-NHFc (A, black line and B, black line), 100 μM ferrocene, 100 μM CuSO₄, and 100 μM GSH (B, red line), and 100 μM GSH-NHFc (B, blue line). The red line in panel A displays a control experiment in which the Cu-GSH-NHFc solution was sparged with N_2 instead of O_2 . All solutions also contained 70% MeOH and 30% aqueous 100 mM TBAClO₄.

Heterogeneous Oxygen Reduction Catalysis and Rotating Disk Experiments

We next heterogenized the Cu-GSH-NHFc catalyst on a glassy carbon electrode so that its ORR activity could be evaluated in a completely aqueous electrolyte. Figure 5A shows LSVs in O₂-sparged pH 5.5 buffer of a glassy carbon rotating disk electrode modified with Cu-GSH-NHFc on Vulcan-XC 72 carbon with a Nafion binder. As expected, the ORR current density increases with increasing rotation speed due to enhanced mass transfer at higher rotation speeds.

Through Koutecký-Levich analysis, we calculated the average number of electrons consumed per O2 during catalysis by Cu-GSH-NHFc as a function of pH (Figure 5B, black points and Figure S5). Alternatively, the number of electrons transferred can be converted to Faradaic efficency values for H₂O production (Figure S6). Within experimental error, Cu-GSH-NHFc reduces O₂ through a four electron pathway at pH values of 4.0, 5.5, and 7.0, which for most applications, such as fuel cells, is desirable. In contrast, at pH values of 2.5, 8.5, and 10.0, Cu-GSH-NHFc catalyzes the ORR with an average of less than four electrons per O₂. These results indicate that at pH values outside the 4-7 range, Cu-GSH-NHFc generates a significant fraction of H₂O₂ during the ORR. Because these two pH regimes correspond well with the pK_a values of glutathione, we hypothesize that protonation and deportonation events of glutathione outside of the pH 4-7 range cause the Cu coordination environment in Cu-GSH-NHFc to change in a manner that is less amenable to the four electron reduction pathway. Assuming similar pK_a values for unmodified GSH as compared to GSH-NHFc, the relevant pK_a values are 2.12 for the carboxylic acid, 8.66 for the primary amine, and 9.62 for the thiol.³⁶ Therefore, at pH values from 4-7, GSH-NHFc will be zwitterionic. In contrast, a large fraction of GSH-NHFc molecules will be cationic or anionic at pH values of 2.5 or 8.5 and 10.0, respectively. As is observed here,

protonation events of other ORR catalysts comprised of Cu complexes of nitrogen-containing ligands dramatically affect ORR activity. 37,38

We also compared the number of electrons transferred during ORR by Cu-GSH-NHFc to Cu-GSH (Figure 4B, red points and Figure S7), the latter of which does not contain the appended ferrocene moiety. At all pH values tested, Cu-GSH catalyzes the ORR with an average of less than four electrons per O₂. This finding indicates that the covalently attached ferrocene moeity in Cu-GSH-NHFc is instrumental in enabling the catalyst to reduce O₂ by four electrons and avoid the production of H₂O₂. All of the conclusions obtained from the rotating disk electrode experiments were also confirmed with rotating ring-disk experiments, which were also used to calculated the average number of electrons transferred per O₂ consumed. The trends in the calculated number of electrons transferred using rotating ring-disk experiments were similar to those calculating using rotating disk experiments (Figures S8-S10). In addition to the rotating disk and rotating ring-disk experiments, we also confirmed the production of H₂O₂ using dye-based spectroelectrochemistry (Figure S11).

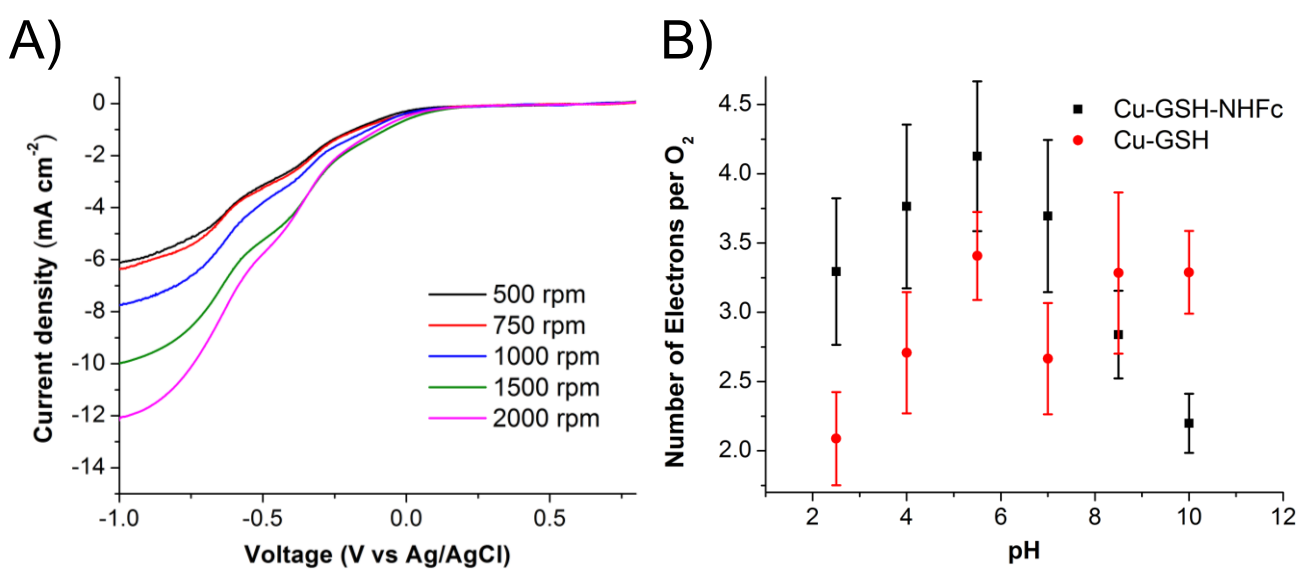


Figure 5: Electrocatalytyic O₂ reduction by Cu-GSH-NHFc at pH 5.5 on a rotating disk electrode at 10 mV s⁻¹ at different rotation speeds (A). Number of electrons transferred per O₂

consumed using Cu-GSH-NHFc (black points) and Cu-GSH (red points) catalysts as determined by Koutecký-Levich analysis from rotating disk electrochemistry (B).

Reaction Pathway of Oxygen Reduction by Cu-GSH-NHFc and Cu-GSH

We now discuss a possible rationalization for why the ferrocene moiety in Cu-GSH-NHFc allows the catalyst to favor the four-electron pathway for the ORR. A careful analysis of the literature describing molecular Cu ORR catalysts reveals that multinuclear (typically dinuclear) Cu centers are involved in catalysts that reduce O₂ via the four-electron pathway.^{21,39} Even catalysts containing nominally mononuclear Cu complexes were later shown to operate via a dinuclear mechanism.⁴⁰ For these reasons, we propose that the Cu complexes here also reduce O₂ via a dinuclear Cu center, but studies in our laboratory are ongoing to further interrogate this point.

In order to propose a reaction pathway, it is useful to determine the stoichiometry of Cu-GSH-NHFc. By collecting UV-visible absorbance spectra across different molar ratios of Cu ions and GSH-NHFc, we used Job plot analysis to determine that in Cu-GSH-NHFc, Cu and the GSH-NHFc ligand exist in a 1:1 molar ratio (Figure S12). This Job plot analysis was also confirmed by ICP-MS analysis, which shows that the Cu:Fe ratio is 0.98:1, close to the expected 1:1 value. Similar UV-vis experiments with Cu-GSH also suggest a 1:1 molar ratio between Cu and the ligand (Figure S13). Although there is debate over the Cu coordination environment in Cu-GSH, ^{24,25,41} most studies suggest involvement of the carboxylate and amine moieties of the glutamate residue and/or the thiol group. Our finding that a 1:1 Cu to ligand stoichiometry exists in both Cu-GSH and Cu-GSH-NHFc is consistent with the Cu in Cu-GSH-NHFc having an analogous coordination environment as in Cu-GSH, especially when considering that the Fc is attached via the pendant glycine residue. In biological contexts, Cu-GSH has been shown to chemically react with O₂ to form Cu complexes of oxidized glutathione (Cu-GSSG). ^{41,42} A

further set of experiments with Cu and oxidized glutathione demonstrates that under our conditions, the Cu:GSSG ratio is 2:1 in the Cu-GSSG complex (Figure S14). Because this stoichiometry is different from those found for Cu-GSH and Cu-GSH-NHFc, this finding suggests that within the time scale of our experiments, the GSH in Cu-GSH-NHFc is not chemically oxidized by dissolved O₂ to form GSSG. In other words, the GSH moiety is stable within Cu-GSH-NHFc and does not form GSSG, at least in the absence of any electrochemistry.

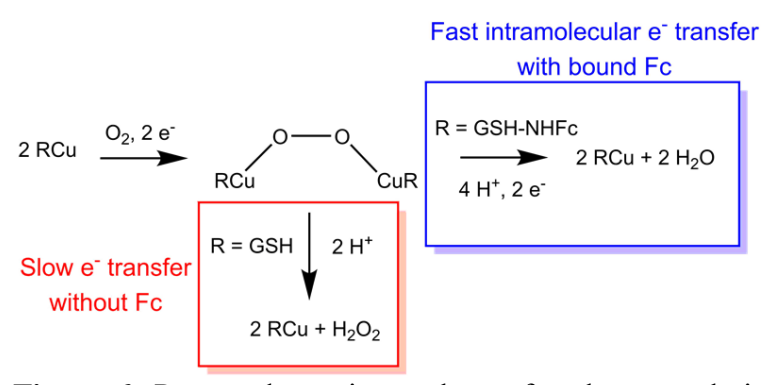


Figure 6: Proposed reaction pathway for electrocatalytic O₂ reduction by Cu-GSH-NHFc and Cu-GSH.

Based on these findings and previous dinuclear Cu ORR mechanisms^{34,43} we propose a reaction pathway for ORR by both Cu-GSH-NHFc and Cu-GSH (Figure 6). First, two Cu-containing complexes react with O₂ to form a dimeric Cu-O-O-Cu intermediate in a two-electron transfer step. When electron transfer is relatively rapid, further electron transfer can occur to yield the four-electron product, H₂O (blue box). We hypothesize that the covalently bound ferrocene moieties increase electron transfer rates to the Cu active site, thus explaining why Cu-GSH-NHFc is capable of catalyzing the ORR by four electrons. In contrast, without the appended ferrocene groups, the electron transfer rates to the Cu active site are slower. In this case, protonation of the Cu-O-O-Cu intermediate occurs as a side reaction, which results in the formation of the two-electron product, H₂O₂ (red box). This production of H₂O₂ at relatively

slow electron transfer rates explains why Cu-GSH does not reduce O₂ by four electrons regardless of the pH. Our finding that covalently attached ferrocene groups can improve the ORR catalyzed by Cu complexes is similar to previous work demonstrating that ferrocene-modified Fe porphyrins also catalyze the ORR by four electrons.⁴⁴

We view using ferrocene to accelerate electron transfer as a complimentary approach to previous studies in which the rates of proton transfer were decreased to dinuclear Cu ORR catalysts using membranes.⁴³ In these studies, the slower proton transfer rates are thought to decrease the rates of protonating the Cu-O-O-Cu intermediate, thus avoiding the production of H_2O_2 (red box) Here, with a ferrocene-modified Cu ORR catalyst, the opposite approach is taken whereby faster electron transfer rates favor O-O bond breaking (blue box), which also avoids H_2O_2 production and yields a catalyst that selectively produces H_2O .

Conclusions

We synthesized Cu complexes of glutathiones and evaluated their catalytic activity

towards ORR. CV studies demonstrate that intermolecular electron transfer in Cu-GSH-NHFc

occurs between Cu and the Fe in the ferrocene-modified glutathione ligand. Homogeneous

catalysis results show that Cu, GSH and ferrocene by themselves do not have the same ORR

activity as Cu-GSH-NHFc, thus proving the utility of covalently binding these components

together. In other words, although the Cu center is presumed to be the active site of the catalyst,

the nature of GSH-NHFc enables its superior ORR activity. Rotating disk electrode and rotating

ring-disk electrodes experiments indicate that Cu-GSH-NHFc catalyzes the ORR through a four-

electron pathway at pH 4.0-7.0, while the Cu-GSH catalyst without the appended ferrocene

catalyzes the ORR with less than four electrons regardless of pH. These findings imply that the

attached ferrocene in Cu-GSH-NHFc is instrumental in the catalyst's ability to reduce O₂ to H₂O.

We propose a reaction pathway based on competing rates of proton and electron transfer events

that is consistent with these findings. We anticipate that this understanding will contribute to the

development of future non-precious metal ORR catalysts based on rational design rules.

Author Information

Corresponding Author

*E-mail: cbarile@unr.edu

Notes

The authors declare no competing financial interest.

16

Supporting Information

Additional cyclic voltammetry data, Randles-Sevcik plots, rotating disk electrochemistry data, rotating ring-disk electrochemistry data, UV-visible spectroscopy data, and Job plots.

Acknowledgments

This material is based upon work supported by the National Science Foundation CAREER Award under Grant No. CHE-2046105. We acknowledge the Shared Instrumentation Laboratory in the Department of Chemistry at UNR.

References

- (1) Liu, T.; Zhou, Z.; Guo, Y.; Guo, D.; Liu, G. Block Copolymer Derived Uniform Mesopores Enable Ultrafast Electron and Ion Transport at High Mass Loadings. *Nat. Commun.* **2019**, *10*, 1-10.
- (2) Wu, G.; Santandreu, A.; Kellogg, W.; Gupta, S.; Ogoke, O.; Zhang, H.; Wang, H.-L.; Dai, L. Carbon Nanocomposite Catalysts for Oxygen Reduction and Evolution Reactions: From Nitrogen Doping to Transition-Metal Addition. *Electrocatalysis* **2016**, *29*, 83-110.
- (3) Faustini, M.; Giraud, M.; Jones, D.; Rozière, J.; Dupont, M.; Porter, T. R.; Nowak, S.; Bahri, M.; Ersen, O.; Sanchez, C. Hierarchically Structured Ultraporous Iridium-Based Materials: A Novel Catalyst Architecture for Proton Exchange Membrane Water Electrolyzers. *Adv. Energy Mater.* **2019**, *9*, 1802136-1802146.
- (4) Jaouen, F.; Proietti, E. M. Lef Vre, R. Chenitz, J. P. Dodelet, G. Wu, H. T. Chung, C. M. Johnston, P. Zelenay. Recent Advances in Non-precious Metal Catalysis for Oxygen-reduction Reaction in Polymer Electrolyte Fuel Cells. *Energy Env. Sci* **2011**, *4*, 114-130.
- (5) Costentin, C.; Drouet, S.; Passard, G.; Robert, M.; Savéant, J. M. Proton-Coupled Electron Transfer Cleavage of Heavy-Atom Bonds in Electrocatalytic Processes. Cleavage of a C–O Bond in the Catalyzed Electrochemical Reduction of CO₂. J. Am. Chem. Soc. **2013**, 135, 9023-9031.
- (6) Fan, L.; Xia, C.; Yang, F.; Wang, J.; Wang, H.; Lu, Y. Strategies in Catalysts and Electrolyzer Design for Electrochemical CO₂ Reduction toward C2+ Products. *Sci. Adv.* **2020**, *6*, eaay3111-eaay3127.
- (7) Le, J. M.; Alachouzos, G.; Chino, M.; Frontier, A. J.; Lombardi, A.; Bren, K. L. Tuning Mechanism through Buffer Dependence of Hydrogen Evolution Catalyzed by a Cobalt Mini-Enzyme. *Biochemistry* **2020**, *59*, 1289-1297.
- (8) Yeager, E. Electrocatalysts for O₂ Reduction. *Electrochim. Acta* **1984**, *29*, 1527-1537.
- (9) Chen, Z.; Higgins, D.; Yu, A.; Zhang, L.; Zhang, J. A Review on Non-Precious Metal Electrocatalysts for PEM Fuel Cells. *Energy Environ. Sci.* **2011**, *4*, 3167-3192.
- (10) Jones, S. M.; Solomon, E. I. Electron Transfer and Reaction Mechanism of Laccases. *Cell. Mol. Life Sci.* **2015**, *72*, 869-883.

- (11) Varnell, J. A.; Edmund, C. M.; Schulz, C. E.; Fister, T. T.; Haasch, R. T.; Timoshenko, J.; Frenkel, A. I.; Gewirth, A. A. Identification of Carbon-Encapsulated Iron Nanoparticles as Active Species in Non-Precious Metal Oxygen Reduction Catalysts. *Nat. Commun.* **2016**, 7, 1-9.
- (12) Kramm, U. I.; Herranz, J.; Larouche, N.; Arruda, T. M.; Lefevre, M.; Jaouen, F.; Bogdanoff, P.; Fiechter, S.; Abs-Wurmbach, I.; Mukerjee, S. Structure of the Catalytic Sites in Fe/N/C-Catalysts for O 2-Reduction in PEM Fuel Cells. *Phys. Chem. Chem. Phys.* **2012**, *14*, 11673-11688.
- (13) Lv, H.; Li, D.; Strmcnik, D.; Paulikas, A. P.; Markovic, N. M.; Stamenkovic, V. R. Recent Advances in the Design of Tailored Nanomaterials for Efficient Oxygen Reduction Reaction. *Nano Energy* **2016**, *29*, 149-165.
- (14) Shao-Horn, Y.; Sheng; W. C.; Chen, S.; Ferreira, P. J.; Holby, E. F.; Morgan, D. Instability of Supported Platinum Nanoparticles in Low-Temperature Fuel Cells. *Top. Catal.* **2007**, *46*, 285-305.
- (15) Yang, X.; Roling, L. T.; Vara, M.; Elnabawy, A. O.; Zhao, M.; Hood, Z. D.; Bao, S.; Mavrikakis, M.; Xia, Y. Synthesis and Characterization of Pt-Ag Alloy Nanocages with Enhanced Activity and Durability toward Oxygen Reduction. *Nano Lett.* **2016**, *16*, 6644-6649.
- (16) Choi, C. H.; Lim, H.-K.; Chung, M. W.; Chon, G.; Sahraie, N. R.; Altin, A.; Sougrati, M.-T.; Stievano, L.; Oh, H. S.; Park, E. S. The Achilles' Heel of Iron-Based Catalysts during Oxygen Reduction in an Acidic Medium. *Energy Environ. Sci.* **2018**, *11*, 3176-3182.
- (17) Tse, E. C.; Schilter, D.; Gray, D. L.; Rauchfuss, T. B.; Gewirth, A. A. Multicopper Models for the Laccase Active Site: Effect of Nuclearity on Electrocatalytic Oxygen Reduction. *Inorg. Chem.* **2014**, *53*, 8505-8516.
- (18) Thiyagarajan, N.; Janmanchi, D.; Tsai, Y. F.; Wanna, W. H.; Ramu, R.; Chan, S. I.; Zen, J. M.; Yu, S. S. F. A Carbon Electrode Functionalized by a Tricopper Cluster Complex: Overcoming Overpotential and Production of Hydrogen Peroxide in the Oxygen Reduction Reaction. *Angew. Chem.* **2018**, *130*, 3674-3678.
- (19) Artyushkova, K.; Serov, A.; Rojas-Carbonell, S.; Atanassov, P. Chemistry of Multitudinous Active Sites for Oxygen Reduction Reaction in Transition Metal-Nitrogen-Carbon Electrocatalysts. *J. Phys. Chem. C* **2015**, *119*, 25917-25928.
- (20) Pegis, M. L.; Martin, D. J.; Wise, C. F.; Brezny, A. C.; Johnson, S. I.; Johnson, L. E.; Kumar, N.; Raugei, S.; Mayer, J. M. Mechanism of Catalytic O₂ Reduction by Iron Tetraphenylporphyrin. *J. Am. Chem. Soc.* **2019**, *141*, 8315-8326.
- (21) Fonseca, S.; de Campos Pinto, L. M. Oxygen Reduction Reaction on a Cu(II) Complex of 3,5-Diamino-1, 2, 4-Triazole: A DFT Approach. *ACS Omega* **2020**, *5*, 1581-1585.
- (22) Cui, L.; Cui, L.; Li, Z.; Zhang, J.; Wang, H.; Lu, S.; Xiang, Y. A Copper Single-Atom Catalyst towards Efficient and Durable Oxygen Reduction for Fuel Cells. *J. Mater. Chem. A* **2019**, *7*, 16690-16695.
- (23) Bhagi-Damodaran, A.; Michael, M. A.; Zhu, Q.; Reed, J.; Sandoval, B. A.; Mirts, E. N.; Chakraborty, S.; Moënne-Loccoz, P.; Zhang, Y.; Lu, Y. Why Copper Is Preferred over Iron for Oxygen Activation and Reduction in Haem-Copper Oxidases. *Nat. Chem.* **2017**, *9*, 257-263.
- (24) Pedersen, J. Z.; Steinkühler, C.; Weser, U.; Rotilio, G. Copper-Glutathione Complexes under Physiological Conditions: Structures in Solution Different from the Solid State Coordination. *Biometals* **1996**, *9*, 3-9.

- (25) Yin, S.-N.; Liu, Y.; Zhou, C.; Yang, S. Glutathione-Mediated Cu(I)/Cu(II) Complexes: Valence-Dependent Effects on Clearance and In Vivo Imaging Application. *Nanomaterials* **2017**, *7*, 132-141.
- (26) Peng, Y.; Liu, Y.-N.; Zhou, F. Voltammetric Studies of the Interactions Between Ferrocene-Labeled Glutathione and Proteins in Solution or Immobilized onto Surface. *Electroanal. Int. J. Devoted Fundam. Pract. Asp. Electroanal.* **2009**, *21*, 1848-1854.
- (27) Wang, C.; Jiang, K.; Xu, Z.; Lin, H.; Zhang, C. Glutathione Modified Carbon-Dots: From Aggregation-Induced Emission Enhancement Properties to a "Turn-on" Sensing of Temperature/Fe³⁺ Ions in Cells. *Inorg. Chem. Front.* **2016**, *3*, 514-522.
- (28) Martos-Maldonado, M. C.; Casas-Solvas, J. M.; Téllez-Sanz, R.; Mesa-Valle, C.; Quesada-Soriano, I.; García-Maroto, F.; Vargas-Berenguel, A.; García-Fuentes, L. Binding Properties of Ferrocene-Glutathione Conjugates as Inhibitors and Sensors for Glutathione S-Transferases. *Biochimie* **2012**, *94*, 541–550.
- (29) Mitamura, K.; Sogabe, M.; Sakanashi, H.; Watanabe, S.; Sakai, T.; Yamaguchi, Y.; Wakamiya, T.; Ikegawa, S. Analysis of Bile Acid Glutathione Thioesters by Liquid Chromatography/Electrospray Ionization—Tandem Mass Spectrometry. *J. Chromatogr. B* **2007**, *855*, 88-97.
- (30) Vollhardt, K. P. C.; Schore, N. E. *Organic Chemistry: Structure and Function*, 5th ed.; W. H. Freeman and Company, 2007.
- (31) Collman, J. P.; Devaraj, N. K.; Decreau, R. A.; Yang, Y.; Yan, Yi-Long; Ebina, W.; Eberspacher, T. A.; Chidsey, C. E. D. A Cytochrome c Oxidase Model Catalyzes Oxygen to Water Reduction Under Rate-Limiting Electron Flux. *Science* **2007**, *315*, 1565-1568.
- (32) Collman, J. P.; Dey, A.; Barile, C. J.; Ghosh, S.; Decreau, R. A. Inhibition of Electrocatalytic O₂ Reduction of Functional CcO Models by Competitive, Non-Competitive, and Mixed Inhibitors. *Inorg. Chem.* **2009**, *48*, 10528-10534.
- (33) Bojang, A. A.; Wu, H. S. Characterization of Electrode Performance in Enzymatic Biofuel Cells Using Cyclic Voltammetry and Electrochemical Impedance Spectroscopy. *Catalysts* **2020**, *10*, 782-801.
- (34) Thorseth, M. A.; Tornow, C. E.; Edmund, C. M.; Gewirth, A. A. Cu Complexes That Catalyze the Oxygen Reduction Reaction. *Coord. Chem. Rev.* **2013**, *257*, 130-139.
- (35) Barile, C. J.; Edmund, C. M.; Li, Y.; Sobyra, T. B.; Zimmerman, S. C.; Hosseini, A.; Gewirth, A. A. Proton Switch for Modulating Oxygen Reduction by a Copper Electrocatalyst Embedded in a Hybrid Bilayer Membrane. *Nat. Mater.* **2014**, *13*, 619-623.
- (36) Pirie, N. W.; Pinhey, K. G. The Titration Curve of Glutathione. *J. Biol. Chem.* **1929**, *84*, 321-333.
- (37) Thorseth, M. A.; Letko, C. S.; Tse, E. C.; Rauchfuss, T. B.; Gewirth, A. A. Ligand Effects on the Overpotential for Dioxygen Reduction by Tris (2-Pyridylmethyl) Amine Derivatives. *Inorg. Chem.* **2013**, *52*, 628-634.
- (38) Zeng, T.; Wu, H.-L.; Li, Y.; Edmund, C. M.; Barile, C. J. Physical and Electrochemical Characterization of a Cu-Based Oxygen Reduction Electrocatalyst inside and Outside a Lipid Membrane with Controlled Proton Transfer Kinetics. *Electrochim. Acta* **2019**, *320*, 134611-134623.
- (39) Liu, C.; Lei, H.; Zhang, Z.; Chen, F.; Cao, R. Oxygen Reduction Catalyzed by a Water-Soluble Binuclear Copper(II) Complex from a Neutral Aqueous Solution. *Chem. Commun.* **2017**, *53*, 3189-3192.

- (40) McCrory, C. C.; Devadoss, A.; Ottenwaelder, X.; Lowe, R. D.; Stack, T. D. P.; Chidsey, C. E. Electrocatalytic O₂ Reduction by Covalently Immobilized Mononuclear Copper (I) Complexes: Evidence for a Binuclear Cu₂O₂ Intermediate. *J. Am. Chem. Soc.* **2011**, *133*, 3696-3699.
- (41) Speisky Cosoy, H.; López Alarcón, C.; Olea Azar, C.; Sandoval-Acua, C.; Aliaga, M. E. Role of Superoxide Anions in the Redox Changes Affecting the Physiologically Occurring Cu(I)-Glutathione Complex. *Bioinorg. Chem. Appl.* **2011**, *2011*, 1-8.
- (42) Ngamchuea, K.; Batchelor-McAuley, C.; Compton, R. The Copper (II)-Catalyzed Oxidation of Glutathione. *Chem. Eur. J.* **2016**, *22*, 1-16.
- (43) Edmund, C. M.; Barile, C. J.; Kirchschlager, N. A.; Li, Y.; Gewargis, J. P.; Zimmerman, S. C.; Hosseini, A.; Gewirth, A. A. Proton Transfer Dynamics Control the Mechanism of O₂ Reduction by a Non-Precious Metal Electrocatalyst. *Nat. Mater.* **2016**, *15*, 754-759.
- (44) Samanta, S.; Sengupta, K.; Miitra, K.; Bandyopadhyay, S; Dey, A. Selective Four Electron Reduction of O₂ by an Iron Porphyrin Electrocatalyst under Fast and Slow Electron Fluxes. *Chem. Commun.* **2012**, *48*, 7631-7633.

TOC Graphic

